

X-ray and Microwave Signatures of Coronal Mass Ejections

N. GOPALSWAMY*

The Catholic University of America and NASA Goddard Space Flight Center, Greenbelt, MD 20771, USA

E-mail: gopals@fugee.gsfc.nasa.gov

Abstract

X-ray and microwave imaging of structures associated with coronal mass ejections (CMEs) have provided a wealth of new information towards a better understanding of solar eruptions. I review the recent research based on microwave imaging from the Nobeyama Radioheliograph and X-ray imaging from the *Yohkoh* Soft X-ray Telescope. I shall discuss the advances made towards understanding the near surface manifestations of CMEs best observed in X-rays and microwaves. In particular, I discuss (i) observability of CMEs in X-rays and microwaves, (ii) coronal dimming, (iii) relation between CME substructures, (iv) heating and expansion of eruptive prominences, (v) timing of flare, CME and prominence eruptions, and (vi) CME mass estimates from non-optical observations.

Key words: Sun: CMEs — Sun: Prominence eruptions — Sun: Radio radiation

1. Introduction

Coronal mass ejections (CMEs) have been extensively studied since their discovery in the early 1970s (Tousey, 1973) primarily using white light coronagraphic data. The coronagraphs detect the Thomson-scattered photospheric light which is about a million times weaker than the direct photospheric light. To detect such a weak signal, the coronagraphs employ an occulting disk to block the direct sunlight which causes some restrictions on the observability of CMEs: (i) the occulting disk blocks an area larger than the solar disk, so we miss information on where the CMEs are rooted on the Sun, (ii) because of the occulting disk, CMEs occurring on the disk (Earth-directed) are not very well observed, and (iii) the Thomson-scattered signal is strongest when the CME is in the plane of the sky and hence produces a biased sample of CMEs. In the past, information on the near surface manifestations of CMEs could be obtained mainly from H α spectroheliograms which show eruptive prominences and two-ribbon flares. We now know that both of these phenomena provide only partial information on CMEs; we need multiwavelength observations to get a complete picture of the CME onset and early evolution. Microwave, EUV, and X-ray observations of CMEs can be very useful for this purpose because they do not have the limitation of occulting disks and they can observe eruptions at any longitude. Plasmas of different temperatures are involved in these eruptions and one has to use instruments sensitive to a wide range of temperatures (a few $\times 10^3$ K for prominences to several $\times 10^6$ K for flares). There are a number of dedicated solar instruments at present – both ground based and spaceborne – that provide new information on CMEs. Phenomena such as coronal dimming, coronal Moreton waves and coronal arcade formations have now become closely associated with CMEs and have provided several new insights into the CME process; I review some of the recent advances in the study of CMEs in microwave, EUV and X-ray wavelengths.

2. Observational Signatures of CMEs

A white light CME typically consists of a bright frontal structure followed by a dark cavity and a prominence core (see Fig. 1) and the eruption often results in the formation of bright arcades on the solar surface under the span of the CME, observed best in X-rays (Sheeley et al, 1975, Webb et al, 1976; Kahler, 1977; McAllister et al, 1992; Hiei et al, 1993; Kano, 1994; Svestka et al, 1995; Khan et al, 1997) and in EUV (Gopalswamy et al, 1999b). The microwave instruments are sensitive to the eruptive prominence cores and on occasions detect the arcade formation (Hanaoka et al, 1994; Gopalswamy and Hanaoka, 1998).

* NAS/NRC Senior Research Associate.

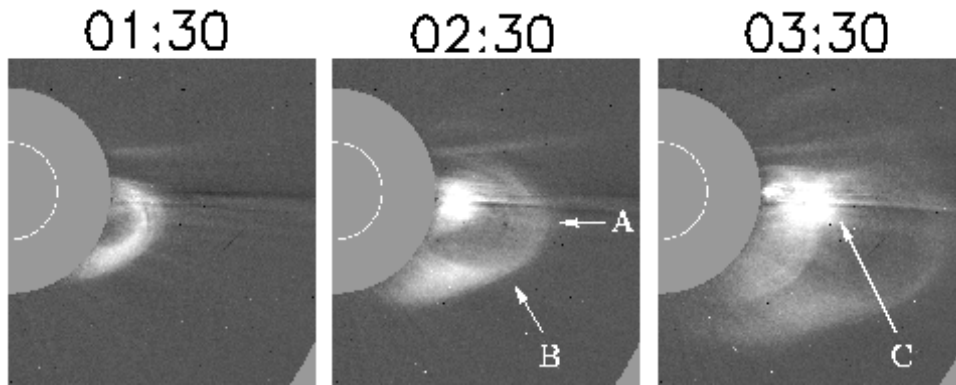


Fig. 1.. A white light CME observed on 1997 February 6–7 by the SOHO/LASCO. A is the frontal structure. The southern leg (B) suggests that the CME had an arcade structure. C is the bright prominence core. The void between A and C is the coronal cavity.

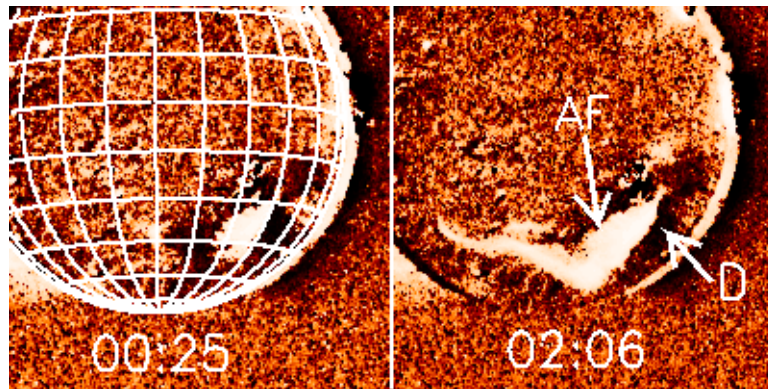


Fig. 2.. Dimming (D) and arcade formation (AF) observed by *Yohkoh*/SXT during the 1997 February 6–7 CME (see Fig.1).

In early studies using *Yohkoh* SXT (Tsuneta et al, 1991) data, there was some confusion in identifying the substructures of a CME (Watanabe et al, 1994; Sime et al, 1994). Klimchuk et al (1994) studied a set of 29 soft X-ray eruptions whose relationship with white light CMEs was not clear. Recently, Webb (1998) found that only 4 out of these 29 eruptions had white light counterparts, although some white light CMEs could have been missed. These early studies concentrated primarily on the prominence core and arcade formation, based on which Hundhausen (1997) concluded that (i) the frontal structure and the legs of a CME, so prominent in white light, are never observed in X-rays, (ii) the coronal dimming may be an early CME signature (base of the white light CME), and (iii) the X-ray arcade formation does not represent a thermal driver for the CME. These conclusions touch upon some crucial issues of CMEs, especially in their onset phase. We shall discuss these issues with illustrative examples from recent investigations. We shall show that the frontal structure and the legs of the CMEs can indeed be observed in X-rays.

2.1. Coronal Dimming as a CME signature

The term “coronal dimming” is presently used to represent the reduction in brightness in a certain region of the corona as compared to an earlier period. The dimming therefore corresponds to a change in the physical conditions of the emitting plasma. Plasma density and temperature are the two important parameters that affect the emission intensity. For a CME signature, one would expect a change in density due to depletion of emitting material in the region of interest.

The coronal dimming in X-rays was first recognized in the *Skylab* images (Webb et al, 1976; Rust and Hildner, 1976) and were also referred to as transient coronal holes appearing astride the X-ray arcade formations (Rust,

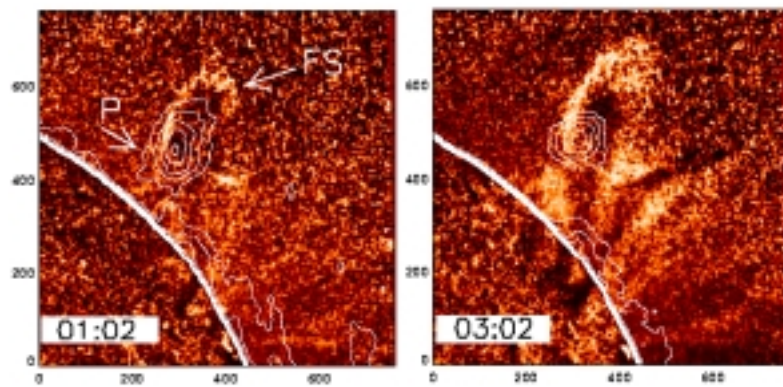


Fig. 3.. The 1993 July 11 CME with frontal structure in X-rays (FS) prominence core (P–17 GHz contour) and the cavity in between. The axes are in units of arcsec.

1983). The work of Rust and Hildner (1976) essentially demonstrated what one would expect of a CME event in X-rays. These authors used the ratio of pre-event and event images to identify the expansion of coronal structures. There is renewed interest in coronal X-ray dimming due to the availability of a large volume of X-ray images from the *Yohkoh/SXT* (see Hudson and Webb, 1997 for a review). The original description used by Rust and Hildner (1976) that the dimming appears on either side of the X-ray arcade is consistent with the idea that the CME is a large scale structure overlying the neutral line. The various manifestations of the dimming, such as cloud ejections, enveloping dimming and transient coronal holes are expected because CMEs come in different sizes and shapes. The dimming signature is best seen in difference images obtained by subtracting a base (pre-event) image from the event images. Fig. 2 shows the dimming region associated with the 1997 February 06-07 CME event. Note that the arcade formation occupies a region within the larger dimming region. There are two issues one must be aware of before using the dimming signature: the role of coronal cavity and the expanding arcade formations. The coronal cavity usually exists in the pre-eruption stage (see e.g. Engvold, 1988) and expands during the eruption. The cavity overlies the filament and the X-ray arcade, and hence may appear similar to the dimming. The frontal structure overlies the cavity and therefore the dimming can include the cavity region also. The contribution of the cavity to the dimming depends on the viewing angle as discussed in detail by Gopalswamy and Hanaoka, (1998).

The dimming signature is also extensively observed in extreme ultraviolet (EUV, see e.g., Thompson et al, 1998; Gopalswamy et al, 1998c; Zarro et al, 1999) by SOHO's Extreme Ultraviolet Imaging Telescope (EIT, Delaboudiniere, 1995). The cadence of EIT images was sufficient to observe the dimming are obtained in 195 Å corresponding to a temperature of ~ 1.5 MK. Since the EIT is sensitive to lower temperature plasma, they often show greater details of the dimming. One has to be careful because when the temperature of the erupting plasma changes sufficiently to values outside the EIT pass band, the plasma may appear darker. This is usually not a serious problem because one can compare with images in other EIT pass bands or observations at other wavelengths such as X-rays and microwaves to eliminate this possibility. On rare occasions, it may also be possible to notice dimming in microwaves as a difference in the free-free emission (Gopalswamy, Hanaoka and Hudson, 1999a).

2.2. Observability in X-rays

The observability of CMEs in X-rays depends on a number of factors:

1. Limited dynamic range: The dynamic range on a typical SXT image is ~ 4000 . The soft X-ray flare (or arcade formation) typically has a much larger temperature and emission measure than the frontal structure (which is typically at coronal temperature and of lower density) and can easily mask the weaker structures. Bright regions outside the region of interest may also reduce the observability of weaker frontal structures. The counting statistics limitation (SXT collecting area is only about 1 cm^{-2}) also reduces the observability of the CME frontal structure.

2. Temperature response: The CME frontal structure is typically at a temperature of 1-2 MK. *Yohkoh/SXT* is more sensitive to plasma with temperatures > 3 MK. Thus only under rare circumstances that one can detect the frontal structure. The 1993 July 10-11 CME was one such case where the CME was relatively small and slow from a quiet region and hence could be detected in X-rays. Fig. 3 shows the three part structure of the CME observed by *Yohkoh/SXT* and Nobeyama radioheliograph (Nakajima et al, 1994; Gopalswamy et al, 1996, 1997a).

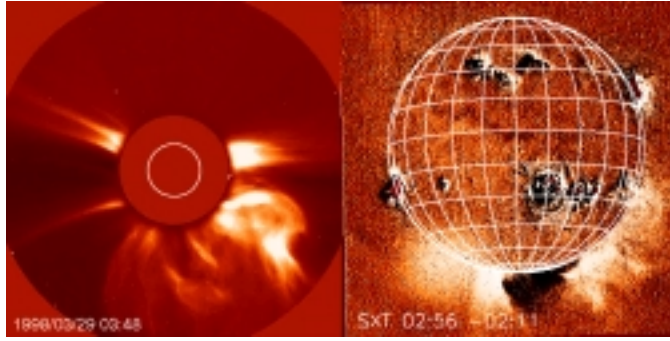


Fig. 4. (left) SOHO/LASCO image of the 1998 March 29 CME at 03:48 UT. The inner white circle represents the optical Sun. The LASCO C2 field of view is bound between the outer circle and the occulting disk at $2 R_{\odot}$. (right) *Yohkoh*/SXT difference image at 02:56 showing a pattern similar to the white light image. The diffuse enhancement at the left end is an artefact. Note that the X-ray and white light brightness have different density dependences.

The temperature of the *Skylab* X-ray arches reported by Rust and Hildner (1976) was in the range 1.5–2.5 MK and hence they were able to detect the frontal structure of the CME.

3. Backside events: When a CME originates from behind the limb, the bright arcade formation and other bright regions on the disk will be occulted so that one can observe the frontal structure in X-rays. Fig. 4 shows the 1998 March 29 CME which occurred from behind the limb probably from the high southern latitudes. The white light CME at 03:48 UT covered a position angle range of $\sim 180^{\circ}$, centered around 200° . The CME was also very fast ($\sim 1500 \text{ km s}^{-1}$). The CME was detected by the *Yohkoh*/SXT as the disappearance of a large scale feature from above the south polar limb. In the X-ray difference image, one can clearly see the depletion of material as well as new material appearing above the limb (see Fig. 4 right). The lateral structure of the white light CME is quite closely reflected in the X-ray images, even though they are at different heights. Note especially the bright-dark-bright pattern as one goes from east to west across the south polar limb. This indeed seems to be the leg of the white light CME.

4. Disk CMEs: Soft X-ray telescopes such as the *Yohkoh*/SXT have a limited field of view above the solar disk and hence larger CMEs can often be missed. So, the X-ray observability increases for disk CMEs. Based on the expectation that eruptive filaments should form the cores of CMEs, and that the arcade formation should be within the CME span, Gopalswamy et al (1999a) searched for CME-like features around the site of the 1993 April 30 filament eruption event. This was a typical eruptive event with a heated strand of the filament moving very fast. Overlying the filament eruption and X-ray arcade formation was a large-scale diffuse X-ray enhancement that very much resembled a CME. The X-ray enhancement roughly covered the entire visible hemisphere of the Sun confirming that the structure was indeed a CME. White light coronagraphs should detect this event as a halo CME, but unfortunately, there was no white light data for this event. In retrospect, we believe that the “cloud dimming” event of Hudson et al (1996) also contained a large scale CME. These authors pointed out that there were large scale global disturbances during the event.

2.3. Observability in Microwaves:

The frontal structure and the filament cavity are coronal features optically thin at microwave frequencies. On the other hand the prominence core is very dense and relatively cool and hence optically thick in microwaves. The arcade formation is a hot coronal structure but of much higher density. The observability of these CME substructures in microwaves can be assessed using the simple formula for free-free optical depth:

$$\tau_{ff} = \alpha \int n^2 dl f^{-2} T^{-3/2}, \quad (1)$$

where $\alpha \sim 0.2$ for $T > 10^4$ and ~ 0.08 for $T < 10^4$, n = electron density, f = observing frequency and T = electron temperature. $\int n^2 dl$ is the emission measure of the structure we are interested in, dl being the elemental length along the line of sight. Let us evaluate the optical depth for various substructures.

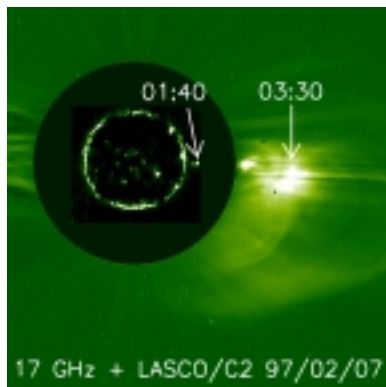


Fig. 5.. Microwave and SOHO/LASCO images of the prominence core of the 1997 February 6–7 CME. The inner bright circle corresponds to solar disk as observed at 17 GHz by the Nobeyama radioheliograph. The 17 GHz prominence at 01:40 was very small compared to the huge one in white light at 03:30 UT suggesting rapid expansion.

The frontal structure and cavity: The typical temperature and density of the frontal structure are 2 MK and $\sim 10^8 \text{ cm}^{-3}$ respectively, so at an observing frequency of 17 GHz, one needs a line of sight depth of $4 \times 10^{14} \text{ cm}$ ($> 10 \text{ AU}$) to make the CME optically thick. If we use a realistic thickness of $\sim 1 R_{\odot}$, equation (1) gives an optical depth of 1.7×10^{-4} and the frontal structure will be at a brightness temperature of only 340 K. The same argument applies to the cavity which is of similar size and lower density and hence the contribution will be still smaller. It must be noted that at meter wavelengths, the conditions are more favorable. At 50 MHz, a CME of $1 R_{\odot}$ thickness will be optically thick and can be readily observed. Such CMEs were observed by radioheliographs at Clark Lake (Gopalswamy and Kundu, 1992; 1993b) and Culgoora (Sheridan et al, 1978). A simulation study by Bastian and Gary (1997) on the detectability of CMEs in microwaves resulted in a similar conclusion.

The prominence/filament core: The cool dense prominence has a large opacity in microwaves: for typical temperature ($\sim 8000 \text{ K}$) and density ($\sim 10^{10-11} \text{ cm}^{-3}$), the prominence core becomes optically thick even for a small line of sight depth of a few km! Hence the prominence core can be readily observed in microwaves as has been demonstrated in a number of recent papers (Hanaoka et al, 1994; Gopalswamy et al, 1996; 1997a; Gopalswamy and Hanaoka, 1998; Gopalswamy, Hanaoka and Hudson, 1999b). Since the corona is optically thin and contributes very little to the microwave brightness temperature, it results in a “cold sky” in microwaves. A prominence observed against the cold sky appears as a bright structure, very similar to a prominence in $H\alpha$. The brightness temperature is typically $\sim 8000 \text{ K}$ at 17 GHz. During eruptive events, the prominence can expand and drain considerably and can become optically thin as shown by Fujiki (1999). Because of the inverse-square frequency dependence of the free-free opacity, the prominence can easily become optically thin at higher frequencies (Irimajiri et al, 1995), although it can remain optically thick at lower frequencies such as 17 GHz. The solar disk (“the microwave quiet Sun”) at 17 GHz has a brightness temperature of $\sim 10^4 \text{ K}$. Therefore the prominence when observed on the disk, appears as a depression (dark filament) with respect to the quiet Sun, by $\sim 2000 \text{ K}$. When the filament erupts, it can often get heated up and becomes indistinguishable from the quiet Sun (“disappears”). The radio disappearance is due to a different physical mechanism compared to the $H\alpha$ disappearance; the latter happens when the filament ceases to absorb the $H\alpha$ line radiation when its temperature increases.

The arcade formation: Hanaoka et al (1994) imaged the arcade formation of the 1992 July 30–31 event in microwaves. The imaging was possible because the free-free emission from the arcade was high enough to be detected in microwaves. From *Yohkoh*/SXT images, the average temperature and density of the arcade were derived to be 3.5 MK and $2.4 \times 10^9 \text{ cm}^{-3}$ respectively. Using the measured size (28000 km) of the arcade at the brightest region as the line of sight depth, equation (1) gives an optical depth of 0.0017 and results in a brightness temperature of $\sim 6000 \text{ K}$, similar to what was observed. After accounting for the difference in spatial resolution of radio and X-ray data, Hanaoka et al (1994) showed that the observed and computed brightness temperatures were in close agreement.

In summary, X-ray and microwave images of CMEs do indeed provide valuable information on the near surface manifestations of CMEs. The combination of X-rays and microwaves has proved to be extremely useful in understanding the early phase of CMEs. The next few sections summarize some of these studies.

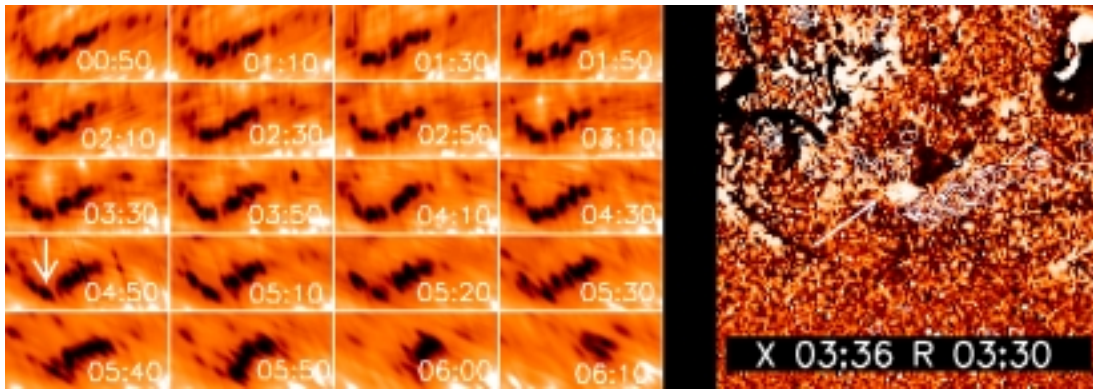


Fig. 6.. (left) The filament eruption of 1998 Jan 21. (right) The filament at 03:30 (radio contour:R) is superposed on an SXT difference image at 03:36 UT (X). Note the triangular depletion and a small brightening denoted by arrow. This is the location from which the filament lifted off.

3. Heating and expansion of prominences

Prominence eruptions are characterized by decreasing density (expansion) and increasing temperature (heating) as functions of time (Illing and Athay, 1986). Prominence cores of CMEs often maintain their structural and physical identity for long distances from the Sun and measurements could be made to distances as far as the edge of SOHO/LASCO C3 field of view at $30 R_{\odot}$. Tracking of the prominence core has helped identify the structure of the magnetic clouds in the interplanetary medium and their relationship to the CME substructures observed in the coronagraph images (Burlaga et al, 1998; Gopalswamy et al, 1998b). Prominence eruptions represent different degrees of heating in different events (Poland and Munro, 1976; Schmahl and Hildner, 1977; Gopalswamy et al, 1997b). The heating of prominences can be sudden as they begin to erupt and may not show much further increase (Hanaoka and Shinkawa, 1999). The early X-ray “spine-brightening” in filaments is a clear indication that the filament heating is one of the earliest signatures of eruptive events (Sheeley et al, 1975; Kahler, 1977; McAllister et al, 1992; Solberg and McAllister, 1998; Gopalswamy et al, 1999b). When the prominence expands and slowly evaporates, the outer skin of the prominence may become invisible in microwaves due to reduction in optical depth. This leads to a reduction in size of the radio prominence. On the other hand, continued heating can cause the filament to expand. Thus a combination of dilution due to expansion (filling factor becomes smaller) and prolonged heating (Gopalswamy et al, 1997a) needs to be considered to understand the evolution of the prominences as they erupt. Fig. 5 shows the comparison between the prominence observed in microwaves (01:40 UT) as compared to the core of the 1997 February 6–7 CME observed in white light (03:30 UT). The expansion of the prominence can be crudely estimated from the radio and white light observations. Volume of the prominence at 01:10 UT was estimated to be $7. \times 10^{28} \text{ cm}^3$ from the microwave images, assuming that it had a depth the same as the width. Similarly, the volume of the prominence core was estimated from the white light observations as at least $1.5 \times 10^{32} \text{ cm}^3$ at 02:30 UT. Thus in about 80 minutes, the prominence volume increased by a factor of 2000! This corresponds to an expansion rate of 64 km s^{-1} . A similar expansion rate seems to be indicated by the line of sight velocities of prominence cores of CMEs measured by SOHO/UVCS (Ciaravella et al, 1997). The prominence started as a small filament fragment on the disk a couple of hours earlier, consistent with this expansion rate. Another important confirmation of the expansion came from the solar wind observations of this event. The size of the filament at 1 AU was estimated from the duration of the pressure pulse ($\sim 3 \text{ hr}$) and the average solar wind speed at the time of the pressure pulse (375 km s^{-1}) as 0.027 AU which corresponds to a volume of $8.7 \times 10^{34} \text{ cm}^3$. Thus the overall increase in volume from the start of the eruption to the time it reached 1 AU is by a factor of 10^8 . The density of the pressure pulse in the solar wind was found to be about 10^2 . Since the typical density of the filament in the pre-eruption state is $\sim 10^{10} \text{ cm}^{-3}$, the drop in density by a factor of 10^8 matched the decrease due to the expansion. This value may be drastically different for the case of prominence eruptions where the prominence drains and only a small fraction of it gets expelled.

Filaments erupting from the disk often show remarkable changes in brightness temperature as a signature of expansion and heating (Gopalswamy, Hanaoka and Lemen, 1998). In Fig. 6 (left) we have shown the evolution of

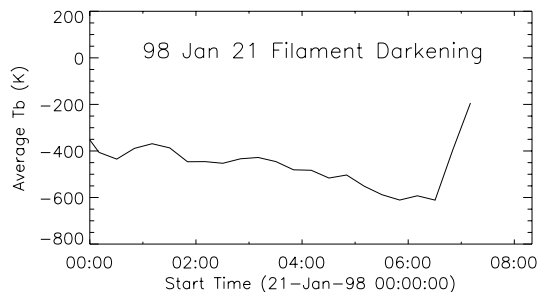


Fig. 7.. Average brightness temperature within a box around the filament of 1998 January 21.

a filament observed in microwaves (17 GHz) over a period of ~ 6 hours. The filament showed rapid change at the location (pointed at by arrow) where the first brightening in X-rays occurred (Fig. 6 right). As the filament erupts, the changes in the filament results in a net increase in the projected area of the filament. The average brightness temperature measured in a box around the eruptive filament often shows a sharp decline and then recovers. The continued darkening of the filament suggests that the filament remains optically thick even though it expands. The “recovery” corresponds to the phase when the filament starts disappearing (due to heating and hence approaching the quiet Sun brightness temperature). The filament might continue to expand, but we cannot observe when it reaches the temperature of the quiet Sun. Fig. 7 shows an example of the filament darkening during the 1998 January 21 CME event. The average brightness temperature with respect to the quiet Sun drops from about -400 K at 00:00 UT (pre-eruption state) by about 50% to -600 K (maximum darkening) and then increases to more than the pre-eruption value (see Fig. 6).

4. Timing of Arcade Formation and Filament Eruptions

The X-ray arcade formation is thought to occur following filament eruptions, but some of the recent observations indicate that the timing is much closer. In many well-observed events, there is always a hint of activity in X-rays the moment we see the filament start to lift (Van Driel-Gesztelyi et al, 1998). The first bright knot of X-ray activity occurs at a break or bend in the neutral line/filament. The filament eruption shown in Fig. 6 (right) had such a behavior. We have shown the contour image of the filament superposed on an X-ray difference image in Fig. 6 (right). A small cusp shaped region showed depletion and a small brightening occurred at the top of this cusp region. EUV observations also show this region as a cusp shaped loop structure. The X-ray arcade formation spread from this initial region and spread on either side to form a huge structure under the span of a halo CME (Gopalswamy et al, 1998a). The cusp (or V) shaped regions are commonly observed as the earliest signature during many eruptions. It needs to be explored further whether these V-shaped structures result from the detachment of filament barbs as proposed by Martin and McAllister (1997).

5. Mass Estimates

An accurate measurement of CME mass is necessary to estimate the CME contribution to the solar wind mass flux. The fact that a single CME accounts for a mass of about a few times 10^{15} g was recognized during early days of CME study (Gosling et al 1974) and was confirmed by further detailed estimates using coronagraph data (Poland et al, 1981; Hildner, 1977; Jackson and Howard, 1993; Webb et al, 1996, Howard et al, 1984). The mass estimate from white light data involves determining the number of electrons in the CME and estimating the CME volume assuming that the CME plasma is fully ionized with 10% helium. Gopalswamy and Kundu (1992; 1993a; 1993b) determined the mass of the 1996 January 16 CME observed by the Clark Lake radioheliograph using thermal free-free emission from the CME. From the observed brightness temperature at a given observing frequency, they determined the electron density assuming a line of sight depth and the coronal temperature. Since they used two dimensional

data, the CME volume could be determined from the projected area of the CME and an assumed line-of-sight depth. They obtained a mass of $\sim 4.2 \times 10^{15}$ g, very similar to the mass of an average CME. Since X-ray emission also originates from the main body of the CME, it should be possible to estimate its mass from X-ray data. The X-ray technique is very similar to the radio one because both are based on the thermal emission properties of the CME plasma. Kahler (1976) showed how to determine the electron density from the *Skylab* X-ray images and the method was successfully applied to the 1973 August 13 CME event by Rust and Hildner (1976) who found the mass loss associated with X-ray depletion to be about 1.3×10^{15} g.

The X-ray images obtained with different filters can be used to determine the temperature and emission measure of the CME plasma which can then be converted to CME mass by estimating the size of the CME. Recently Hudson et al (1996) applied this technique and estimated the mass loss corresponding to the disappearance of a cloud structure to be $\sim 4 \times 10^{14}$ g. Similarly, Gopalswamy et al (1996, 1997a) determined the mass of the 1993 July 10–11 CME to be $\sim 1.2 \times 10^{14}$ g. These values are low, but within the range of values obtained for white light CMEs. The 1993 July 10–11 CME was a small one ($\sim 20^\circ$) compared to a typical CME ($\sim 45^\circ$). Although the mass estimates of Gopalswamy et al (1996, 1997a) and Hudson et al (1996) are similar, the latter authors may have underestimated the mass because of the global changes involved in their event. Sterling and Hudson (1997) estimated the mass from X-ray dimming associated with the 1997 April 07 halo CME and again obtained a mass of a few times 10^{14} g. Gopalswamy and Hanaoka (1998) determined the mass loss corresponding to a well-defined X-ray dimming associated with the eruption of a large prominence to be $\sim 1.7 \times 10^{15}$ g again similar to the typical CME mass. They also estimated that the pre-eruption mass of the prominence was huge ($\sim 6 \times 10^{16}$ g) and the ejected mass in the prominence may be comparable to the frontal mass even after significant draining of the prominence.

5.1. Mass Increase

It must be pointed out that the X-ray and radio mass estimates of CMEs correspond to regions close to the Sun whereas the white light estimates correspond to larger heights (a few solar radii). An interesting question is whether the CME mass increases with height. This was suspected when CME masses from coronagraph data were compared with those from the Helios photometer data (when the CME was in the interplanetary medium). Increases in mass by a factor of up to 3 were found from the corona to the interplanetary medium (Jackson and Howard, 1993; Webb et al, 1996). During the 1993 July 10–11 CME event, it was possible to determine the frontal mass as a function of time over several hours; the result was a large increase in mass (by a factor of 5) over a distance of only $1 R_\odot$ (Gopalswamy et al, 1996, 1997a). The mass increase could be attributed to an increase in volume of the CME frontal structure since the density remained the same. This means that mass addition to the front occurred either through the legs of the CME or through piling up at the top. (The piling-up should be more of a redistribution of the coronal material). Recently, Howard et al (1997) reported mass increase by a factor of 10 when a CME moved from 8 to 15 R_\odot in the SOHO/LASCO field of view. This increase seems to be similar to that reported by Gopalswamy et al (1996, 1997a) and much larger than the average value of 3 reported in Jackson and Howard (1993) and Webb et al (1996). Movies of SOHO/LASCO CMEs clearly show continued mass flow which may be due to new material from the surface on newly opened field lines. The possible coexistence of open and closed field lines in the post-eruption phase due to incomplete reconnection (Klimchuk, 1996) also favors continued outflow of material. Material from the eruptive prominence may also take coronal-like properties and contribute to the mass increase in the frontal structure (Gopalswamy et al, 1996), although this should not change the total mass of the CME. The mass increase may have significant implications to the long-term dynamic evolution of the CMEs. This may also have important consequences to the understanding of the interplanetary manifestations of CMEs such as magnetic clouds and the preceding sheath material (see e.g., Burlaga, 1995; Lepping et al, 1990).

6. X-ray Ejecta and Plasmoids

The concept of isolated plasmoids has been known to the radio astronomers for a long time, as moving type IV bursts at metric wavelengths which are thought to be nonthermal radio emission from plasmoids (Smerd and Dulk, 1971). Only imaging observations can distinguish them from other classes of type IV emissions. These plasmoids were known to be heated prominence material (Wagner, 1984). Gopalswamy and Kundu (1990) tracked an erupting filament and found that it coincided with a moving type IV burst imaged by the Clark Lake radioheliograph. Recently, a moving type IV burst observed by the Nancay radioheliograph was found to be located on an X-ray plasmoid observed by the *Yohkoh*/SXT (Gopalswamy et al, 1997b). Hot plasmoids from flares have also been reported by Ohya and Shibata, (1998) in X-rays and by Shibasaki, (1998) in microwaves. The speeds of these

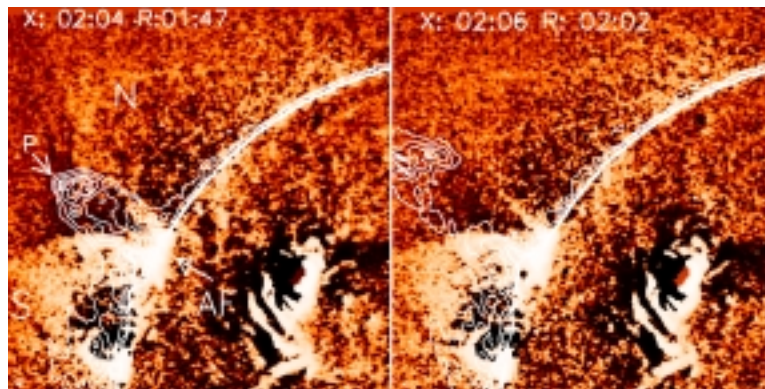


Fig. 8. X-ray (X) and microwave (R) images of the 1993 June 10 eruption at two instances. A base image at 00:14 UT has been subtracted from the X-ray images to show the change. Note the two arcades on the southern (S) and northern (N) sides of the eruptive prominence (P, contour). There is an additional bright arcade (AF) at the bottom of the valley between the two large arcades. Note the brightness enhancement along the edges of the side arcades. The microwave brightness temperature contours are at 500, 1000, 3000, 5000 and 7000 K.

plasmoids could be several hundred km s^{-1} . It is not clear whether these plasmoids are “naked” or they are enclosed by large-scale eruptive structures that could not be observed in X-rays and microwaves due to reasons discussed in earlier sections. Since the ejected prominence material is often seen as the core of CMEs, one expects that these plasmoids are not naked. One has to consider scenarios of eruption involving multiple structures so that fast ejecta can occur not necessarily under the span of the large scale structure, but adjacent to it. Some of the X-ray ejecta were fast enough to drive coronal shocks responsible for metric type II bursts (Gopalswamy et al, 1997b). It is not clear at present whether these ejecta are parts of CMEs “visible” in X-rays or simply fast prominence material heated during the eruption.

7. Multi-Arcade Eruptions

There seems to be no doubt that the CME is a closed magnetic structure, an arcade to be precise. The white light data usually show a simple bipolar structure. However, when we look at the near-surface activities and pre-eruption structures, the picture is rather complex. Several years ago, Uchida (1980) proposed a quadrupolar field configuration in the pre-event stage of arcade formation. Numerical simulations of Biskamp and Welter (1989) also indicated that interaction between multiple arcades favors eruption. These ideas are currently being explored to see if the multi-arcade eruptions are common (Uchida, 1996; Uchida et al, 1998; Webb et al, 1997; Gopalswamy, Hanaoka and Lemen, 1998; Antiochos, 1998). As an illustration, we have shown a prominence eruption observed by the Nobeyama radioheliograph in Fig. 8. When we examined the *Yohkoh*/SXT images, we found that the eruptive filament was located in the valley between two large X-ray arcades (S and N). While the prominence was moving out, there were changes in the two arcades and a new bright arcade (AF) formed close to the solar surface, beneath the prominence in the space between the two arcades. We also note that there was enhanced X-ray emission along the edge of the arcade facing the departing prominence. X-ray images obtained over the next two days suggested that there were indeed multiple neutral lines involved in the eruption region. The situation seems to be somewhat similar to the 1998 January 25 event (Gopalswamy et al, 1999b). Unfortunately, there was no white light CME observation so we do not know whether there was a CME structure overlying the X-ray arcades and the filament or not. However, we can safely say that the post-eruption structure is not a simple bipolar arcade formation. It is also worth noting that these X-ray observations have excellent morphological agreement with the simulation results

of Uchida et al. (1998). Webb et al (1997) found a large number of these events and analyzed five of them to conclude that multiple neutral line eruptions are rather common and seem to be in accordance with energetic requirements of the eruption (see e. g., Aly 1991).

When we view the LASCO coronagraph data in the movie mode, it is easy to recognize cases where the CME starts at high latitude, but is channeled toward the equator as it propagates outward. In the field of view of C3 coronagraph all we see is a streamer blowout event. Fig. 9 shows one such event. Taken alone, the white light

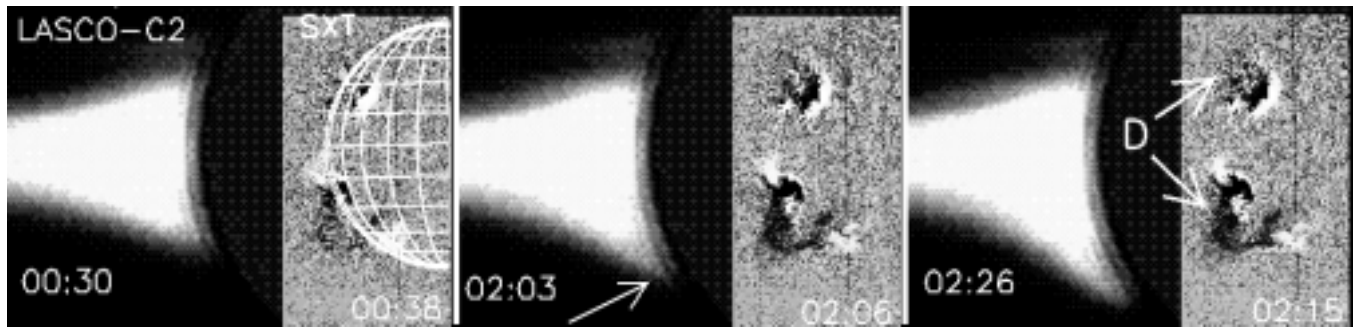


Fig. 9.. A LASCO C2 white light CME event associated with X-ray dimming (D) from *Yohkoh/SXT* on 1997 December 14. Note the distension of the streamer at the location pointed at by arrow. The filament eruption associated with the dimming was in progress radially below the streamer change.

observations indicate a streamer distension, resulting in a huge CME (Gopalswamy, Hanaoka and Hudson, 1999b). A closer look at the activities near the surface revealed a classic quiescent prominence eruption under the southern section of the streamer. There was also a clear dimming signature in X-rays and EUV in the space around the prominence. The streamer swelling occurs first on the southern side, directly above the region of eruption, but eventually the entire streamer structure erupted and the final motion was radially above the equator. Interestingly, there was also a weak X-ray dimming from under the northern leg of the streamer, located symmetric about the equator from the southern dimming region. Taken together with the two dimming regions, the eruption certainly looks like a multi-arcade event.

8. Discussion and Unanswered Questions

The observation by Hundhausen (1997) that there are no X-ray counterparts for frontal structure and legs of a white light CME can be challenged with the available data. In fact a complete CME seems to have been observed in X-rays even during the *Skylab* era (Rust and Hildner, 1976). However, the signals are not as spectacular as one finds in white light data. Hundhausen's second observation that coronal dimming may correspond to the bases of 3-d coronal regions depleted by CMEs is readily confirmed both in X-rays and EUV. The details are somewhat sketchy and more analysis is needed to establish the precise relation between CMEs and dimming.

White light observations of CMES from Mauna Loa Solar Observatory suggest that in the early stage of an eruption, all we see is the cavity. Does this mean all frontal structure is swept up material? But there are a number of events in which the legs are clearly connected to the Sun and are often brighter. X-ray and EUV images of CMEs when compared to SOHO/LASCO data seem to indicate the presence of frontal structure as low as $0.3 R_{\odot}$ above the surface (Gopalswamy et al, 1999b). An alternative explanation of the CME frontal structure is that it is the material swept up by a flare explosion. Although there are claims that the CMEs could be formed out of flare explosions, there is so far no clear evidence.

The post-eruption X-ray arcade seems to be due to reconnection beneath the erupting filament, so the filament and the arcade formation are physically related while both of these are enclosed by a CME. Is this always the case or sometimes the field lines corresponding to the frontal structure reconnect to reform the streamer? Or is the reformed streamer the same as the evolved arcade formation (see e.g., Kahler and Hundhausen, 1992)? What is the scenario when no filament eruption is involved? Reconnection of the frontal field lines has also been proposed as a possible way in which magnetic cloud (flux rope) structures form as the CME propagates towards the interplanetary medium (Gosling, 1990), as opposed to the pre-formed flux ropes before eruption (Low, 1997). A related question is the observational signature of the reconnection flow (Klimchuk, 1996; Hudson et al 1996). If the X-ray arcade formation is due to reconnection, why don't we observe reconnection flows? What is the timing of the reconnection with respect to the eruption?

9. Summary

1) A combination of microwave and X-ray data on solar eruptive events is helpful in arriving at a complete picture of CMEs, especially close to the solar surface. 2) Sometimes it is possible to observe all the substructures (frontal structure, prominence core, cavity and arcade formation) in X-rays. Arcade formation and core are observed most often. 3) The CME core is almost always observed in microwaves. The arcade formation can also be observed most of the times while the frontal structure is least favorable for observation. 4) Filaments heat and expand very close to the surface and can be seen in both microwaves and X-rays. In X-rays, the filament is seen as ‘axial brightening’ while the filament disappears due to lack of contrast with respect to the quiet Sun. 5) Coronal dimming is an important but complex signature of CMEs. Any motion such as active region expansion, arches and arcade evolution can also show dimming. The dimming signatures can be used to estimate the mass loss due to CMEs at their early stages. These estimates may be lower limits to the actual mass. 6) Dimming often precedes filament eruption and the arcade formation occurs at the bottom of the dimming region. Dimming can also precede flares, thus providing independent information on the CME-flare relationship. It must be pointed out that this relationship is not settled, but the new information in X-ray, microwave and EUV wavelengths may shed new light on this issue. 7) Most plasmoid ejections may have overlying structures (CMEs). Hot plasmoids may be the counterparts of filaments with axial brightening. There may be other forms of fast X-ray ejecta that drive coronal shocks. 8) The first instance of filament lift-off seems to be accompanied by X-ray brightening under the filament which eventually becomes the X-ray arcade. The filament may be heated to different temperatures in different events. 9) Streamer disruptions may have complex near-surface manifestations with activities located asymmetrically. There is evidence for multipolar structure under the span of CMEs.

The author thanks S. Kahler, D. Webb and H. Hudson (referee) and S. Kainer for helpful comments. This work was supported by NASA contract NAG-5-6139 and by NSF subcontract from the University of Maryland, College Park. The author greatly benefits from the open data policy of the *Yohkoh* and Nobeyama Radioheliograph teams.

References

- Aly, J. J. 1991, *ApJ*, 375, L61
 Antiochos, S. 1998, *ApJL*, 502, L181
 Bastian, T. S. and Gary, D. E. 1997, *J. Geophys. Res.* 102, 14031
 Biskamp, D. and Welter, H. 1989, *Solar Phys.* 120, 49
 Burlaga, L. F. 1995 in ‘Interplanetary Magnetohydrodynamics’, Oxford University Press, New York, p. 89
 Burlaga, L. F. and 12 co-authors, 1998, *J. Geophys. Res.*, 103, 277
 Ciaravella, A. and 11 co-authors, 1997, *ApJL*, 491, L59
 Delaboudiniere, J.-P., and 27 co-authors, 1995, *Solar Phys.*, 162, 291
 Engvold, O. 1988, in ‘Dynamics and Structure of Quiescent Solar Prominences’, ed. E. R. Priest, Kluwer, Dordrecht, p. 47
 Fujiki, K. 1999, this volume
 Gopalswamy, N. and Hanaoka, Y. 1998, *ApJ*, 498, L179
 Gopalswamy, N., Hanaoka, Y. and Hudson, H. S. 1999a, *ApJL*, to be submitted
 Gopalswamy, N., Hanaoka, Y. and Hudson, H. S. 1999b, *Adv. Space Res.* (in press)
 Gopalswamy, N., Hanaoka, Y. and Lemen, J. R. 1998, in ‘New Perspectives on Solar Prominences,’ ed. D. F. Webb et al., ASP Conf. ser. 150, p. 358
 Gopalswamy, N., Hanaoka, Y., Kaiser, M. L., Gurman, J., Hudson, H. and Howard, R. A. 1998a, in ‘Coronal Explosive Events, ed. S. Pohjolainen, Metsahovi Radio Observatory, p. 40
 Gopalswamy, N., and 11 co-authors, 1998b, *Geophys. Res. Lett.*, 25, 2485
 Gopalswamy, N., Hanaoka, Y., Kundu, M. R., Enome, S., Lemen, J. R., Akioka, M. and Lara, A. 1997a, *ApJ*, 475, 348
 Gopalswamy, N., Kaiser, M. L., MacDowall, R. J., M. J. Reiner, M. J., Thompson, B. J., St. Cyr, O. C. 1998c, in the Proceedings of Solar Wind 9, to be published
 Gopalswamy, N. and Kundu, M. R. 1990, *ApJL*, 365, L31
 Gopalswamy, N. and Kundu, M. R. 1992, *ApJ*, 390, L37
 Gopalswamy, N., and Kundu, M. R. 1993a *Adv Space Res.* 13(9), 95
 Gopalswamy, N., and Kundu, M. R. 1993b, *Solar Phys.* 143, 327
 Gopalswamy, N., Kundu, M. R., Hanaoka, Y., Enome, S., Lemen, J. R. and Akioka, M. 1996, *New Astron.* 1, 207
 Gopalswamy, N., Kundu, M. R., Manoharan, P. K., Nitta, N., and Zarka, P., 1997b, *ApJ*, 486, 1036
 Gopalswamy, N., Nitta, N., Manoharan, P. K., Raoult, A., and Pick, M. 1999a, *Astron. Astrophys.*, in press
 Gopalswamy, N., Yashiro, S., Kaiser, M. L., Thompson, B. J. and Plunkett, S., 1999b, this volume

- Gosling, J., Hildner, E., MacQueen, R. M., Munro, R. H., Poland, A. I., and Ross, C. L. 1974, *J. Geophys. Res.* 79, 4581
- Gosling, J. T. 1990, in 'Physics of Magnetic Flux Ropes', *Geophys. Monogr. Ser.*, Vol. 58, ed. C. T. Russel, E. R. Priest, and L. C. Lee, AGU, Washington DC, p. 343
- Hanaoka, Y. and Shinkawa, T. 1999, *ApJ*, in press
- Hanaoka, Y. and 19 co-authors, 1994, *PASJ*, 46, 205
- Hiei, E., Hundhausen, A. J., and Sime, D. 1993, *J. Geophys. Res.*, 20, 2785
- Hildner, E. 1977, in *Proc of the L. D. de Feiter Memorial Symposium*, Dordrecht, D. Reidel, p. 3
- Howard, R. A., Sheeley, N. R., Jr., Michels, D. J. and Koomen, M. J., 1984, *Adv. Space Res.*, 4(7), 307
- Howard, R. A. and 18 co-authors, 1997, in 'Coronal Mass Ejections', ed. N. Crooker et al, *AGU Monogr.* 99, p. 17
- Hudson, H. S., Acton, L. and Freeland, S. 1996, *ApJ*, 470, 629
- Hudson, H. and Webb, D. F. 1997 in 'Coronal Mass Ejections', ed. N. Crooker et al, *AGU Monogr* 99, p. 27
- Hundhausen, A. J. 1997, in 'Coronal Mass Ejections', ed. N. Crooker et al, *AGU Monogr* 99, p. 1
- Illing, R. M. E. and Athay, R. G. 1986, *Solar Phys.*, 105, 173
- Irimajiri, Y., Takano, T., Nakajima, H., Shibasaki, K., Hanaoka, Y. and Ichimoto, K. 1995, *Solar Phys.*, 156, 363
- Jackson, B. V., and Howard, R. A. 1993, *Solar Phys.*, 148, 359
- Kahler, S. W. 1976, *Solar Phys.*, 48, 255
- Kahler, S. W. 1977, *ApJ*, 214, 891
- Kahler, S. W. and Hundhausen, A. J. 1992, *J. Geophys. Res.*, 97, 1619
- Kano, R. 1994, in 'X-ray Solar Physics from *Yohkoh*', Y. Uchida et al. (eds.), Univ. Acad. Press, Tokyo, p. 273
- Khan, J., Uchida, Y., McAllister, A. H., Mouradian, Z., Soru-Escout, I., and Hiei, E. 1997, *Astron. Astrophys.*, 336, 753
- Klimchuk, J. A. 1996, in 'Magnetic Reconnection in the Solar Atmosphere', ed. R. Bentley and J. Mariska
- Klimchuk, J. A. and 7 co-authors, 1994, in 'X-ray Solar Physics from *Yohkoh*', Y. ed. Uchida et al., Univ. Acad. Press, Tokyo, p. 181
- Lepping, R. L., Burlaga, L. and Jones, J. A. 1990, *J. Geophys. Res.*, 95, 11957
- Low, B. C. 1997, in 'Coronal Mass Ejections', ed. N. Crooker et al, *AGU Monogr* 99, p. 39
- Martin, S. F. and McAllister, A. H. 1997, in 'Coronal Mass Ejections', ed. N. Crooker et al, *AGU Monogr* 99, p. 127
- McAllister, A. and 8 co-authors, 1992, *PASJ*, 44, L205
- Nakajima, H. and 26 co-authors, 1994, *Proc. IEEE*, 82, 705
- Ohyama, M. and Shibata, K. 1998, *ApJ*, 499, 934
- Poland, A. I. and Munro, R. H. 1976, *ApJ*, 209, 927
- Poland, A. I., Howard, R. A., Koomen, M. J., Michels, D. J., and Sheeley, N. R. 1981, *Solar Phys.*, 69, 169
- Rust, D. M. 1983, *Space Sci. Rev.*, 34, 21
- Rust, D. M. and Hildner, E. 1976, *Solar Phys.*, 48, 381
- Schmahl, E. J. and Hildner, E. 1977, *Solar Phys.* 55, 473
- Sheeley, N. R., Jr. and 12 co-authors, 1975, *Solar Phys.*, 45, 377
- Sheridan, K. V., Jackson, B. V., McLean, D. J., and Dulk, G. A. 1978, *Proc. Astron. Soc. Australia*, 3, 249
- Shibasaki, K. 1998, *Metsaehovi Publications on Radio Science*, HUT-MET-27, p. 6
- Sime, D. G., et al. 1994, in 'X-Ray Solar Physics from *Yohkoh*', ed. Y. Uchida et al, Univ Acad Press, Tokyo, p. 197
- Smerd, S. F. and Dulk, G. A. 1971, in 'Solar Magnetic Fields', R. Howard (ed), *IAU Symp.* 43, D. Reidel, p. 616
- Solberg, C. R. and McAllister, A. H. 1998, in 'New Perspectives on Solar Prominences,' ed. D. F. Webb et al., *ASP Conf. ser.* 150, p. 171
- Sterling, A. and Hudson, H. S. 1997, *ApJ*, 491, L55
- Svestka, Z., Farnik, F., Hudson, H. S., Uchida, U., Hick, P. and Lemen, J. R. 1995, *Solar Phys.*, 161, 331
- Thompson, B. J., Plunkett, S. P., Gurman, J. B., Newmark, J. S., St. Cyr, O. C., and Michels, D. J. 1998, *GRL*, 25, 2465
- Tousey, R., *The Solar Corona*, *Adv. Space Res.*, 13, 713, 1973
- Tsuneta, S. and 9 co-authors, 1991, *Solar Phys.*, 136, 37
- Uchida, Y. 1980, in 'Solar Flares', P. A. Sturrock (ed.), University of Colorado Press, Boulder, p. 67
- Uchida, Y. 1996, *Adv. Space Res.*, 17 (4/5), 19
- Uchida, Y. et al. 1998, in 'New Perspectives on Solar Prominences,' ed. D. F. Webb et al., *ASP Conf. ser.* 150, p. 384
- Van Dreil-Gesztelyi, L. and 13 co-authors, 1998, in 'New Perspectives on Solar Prominences,' ed. D. F. Webb et al., *ASP Conf. ser.* 150, p. 366
- Wagner, W. J. 1984, *ARA&A*, 133, 288
- Watanabe, Ta. and 7 co-authors, 1994, in 'X-ray Solar Physics from *Yohkoh*', ed. Y. Uchida et al, Univ. Acad Press, p. 207
- Webb, D. F. 1998, *Physics of Space Plasmas*, in press
- Webb, D. F., Cliver, E. W., Gopalswamy, N., Hudson, H. S., and St. Cyr, O. C., 1998, *Geophys. Res. Lett.*, 25, 2485
- Webb, D. F., Howard, R. A. and Jackson, B. V. 1996, in *Solar Wind 8*, ed. D. Winterhalter et al, *NASA/JPL*
- Webb, D. F., Kahler, S. W., McIntosh, P. S., and Klimchuk, J. A. 1997, *J. Geophys. Res.*, 102, 24161
- Webb, D. F., Krieger, S. and Rust, D. M., 1976, *Solar Phys.*, 48, 159
- Zarro, D. M., Sterling, A. C., Thompson, B. J., and Hudson, H. S., and Nitta, N. 1999, *ApJ*, submitted